

advances.sciencemag.org/cgi/content/full/6/20/eaay9234/DC1

Supplementary Materials for

A hydrodynamic analog of Friedel oscillations

Pedro J. Sáenz*, Tudor Cristea-Platon, John W. M. Bush*

*Corresponding author. Email: saenz@unc.edu (P.J.S.); bush@math.mit.edu (J.W.M.B.)

Published 15 May 2020, *Sci. Adv.* **6**, eaay9234 (2020)
DOI: 10.1126/sciadv.aay9234

The PDF file includes:

Supplementary Text
Figs. S1 and S2
Legends for movies S1 to S5
References

Other Supplementary Material for this manuscript includes the following:

(available at advances.sciencemag.org/cgi/content/full/6/20/eaay9234/DC1)

Movies S1 to S5

Supplementary Text

Effective Force

The drop is drawn into the well through a subtle wave-mediated interaction. However, an analytical expression for the effective well-induced force acting on the drop during the incoming phase, \mathbf{F}_w , may be inferred (23) by exploiting two features evident in both experiments and simulations. First, to a good approximation, the incoming trajectories are Archimedean spirals centered on the well. Second, the drop speed remains constant along these spirals.

By rotating clockwise the walker trajectories (Fig. S1) by their corresponding scattering angles α , all collapse onto an Archimedean spiral (Fig. S2A). Note the nearly linear relationship in $r(\theta)$ (Fig. S2B) and the satisfactory fit to a pure Archimedean spiral (Fig. S2C). The spiral slope $b = dr/d\theta$ decreases in magnitude with increasing drop speed v_0 but remains unaffected by γ/γ_F if drop speed is kept constant (Fig. S2B). Notably, we may accomplish the latter condition with our simulations by readjusting the impact phase (Table 1). In order to deduce an expression for the effective well-induced force, \mathbf{F}_w , we start from the polar form of the drop trajectory, $r(\theta) = a + b\theta$, where (r, θ) are the polar coordinates in the horizontal plane, and a and b are constants that may be determined from the initial conditions. Given the equation of motion $m d\mathbf{v}/dt = \mathbf{F}_w$, where m is the drop mass and $\mathbf{v} = \dot{r}\hat{\mathbf{e}}_r + r\dot{\theta}\hat{\mathbf{e}}_\theta$ in polar coordinates, the well-induced force may be written as

$$\mathbf{F}_w = m \left[\left(\ddot{r} - r\dot{\theta}^2 \right) \hat{\mathbf{e}}_r + \left(r\ddot{\theta} + 2\dot{r}\dot{\theta} \right) \hat{\mathbf{e}}_\theta \right]. \quad (6)$$

Since the drop speed $v = |\mathbf{v}|$ is constant along the incoming spiral, as is the case for $r \gtrsim 2.5\lambda_F$ (Fig. S2B), it follows that

$$v^2 = v_r^2 + v_\theta^2 = \dot{r}^2 + (r\dot{\theta})^2 = \text{const}, \quad (7)$$

an expression whose time derivative yields

$$2\dot{r}\ddot{r} + 2r\dot{r}\dot{\theta}^2 + 2r^2\ddot{\theta} = 0. \quad (8)$$

Noting that $\dot{r} = b\dot{\theta}$ and $\ddot{r} = b\ddot{\theta}$ from the spiral equation, and that $\dot{r} \neq 0$ from (7), we may write

$$\ddot{r} = -\frac{r\dot{\theta}^2}{\left(1 + \frac{r^2}{b^2}\right)}, \quad \text{and} \quad \ddot{\theta} = -\frac{r\dot{\theta}^2}{b\left(1 + \frac{r^2}{b^2}\right)}. \quad (9)$$

By substituting (9) into (6), we deduce the well-induced force:

$$\mathbf{F}_w = m \frac{\left(2 + \frac{r^2}{b^2}\right)}{\left(1 + \frac{r^2}{b^2}\right)} \dot{\theta}^2 (-r\hat{\mathbf{e}}_r + b\hat{\mathbf{e}}_\theta). \quad (10)$$

Using $\dot{r} = b\dot{\theta}$ in (7), it follows that

$$v^2 = \dot{r}^2 \left(1 + \frac{r^2}{b^2}\right). \quad (11)$$

We thus obtain the components of \mathbf{F}_w by substituting (11) and $\dot{r} = b\dot{\theta}$ into (10), which leads to

$$\mathbf{F}_w = m \left(1 + \frac{\dot{r}^2}{v^2}\right) \left(-r\dot{\theta}^2\hat{\mathbf{e}}_r + \dot{r}\dot{\theta}\hat{\mathbf{e}}_\theta\right). \quad (12)$$

Denoting $v_r = \dot{r}$ and $v_\theta = r\dot{\theta}$, we may thus write (12) as

$$\mathbf{F}_w = m \left(1 + \frac{\dot{r}^2}{v^2}\right) \dot{\Theta} \times \mathbf{v}, \quad (13)$$

where $\dot{\Theta} = (v_\theta/r)\hat{\mathbf{e}}_z$ is the drop's instantaneous angular velocity about the well center.

It should be noted that the spiral parameters a and b may be determined from the initial conditions. Denoting the initial position and velocity as (r_0, θ_0) and $(v_{r0}, v_{\theta0})$, respectively, and noting that $\dot{r} = b\dot{\theta}$ may be written as $v_r = bv_\theta/r$ leads to $b = r_0v_{r0}/v_{\theta0}$ and $a = r_0(1 - v_{r0}\theta_0/v_{\theta0})$.

It is interesting to compare the inferred form (13) of the well-induced force with that inferred by Harris *et al.* (23) for walker scattering off a submerged circular pillar. While both are lift forces, acting perpendicular to the walker, the drop is drawn inwards into the well along an Archimedean spiral, and driven outwards by the pillar along a logarithmic spiral. The slightly different forms of these lift forces presumably reflects the different forms of the pilot waves in the two situations. Rationalizing their different forms is left for future consideration.

We conclude by noting that the effective well-induced force may be tuned through the outer fluid depth h . Notably, decreasing h sufficiently may lead to trapped states, in which the drop is unable to escape the well (Fig. S2D), as are known to arise for $\gamma > \gamma_F$ (38–40).

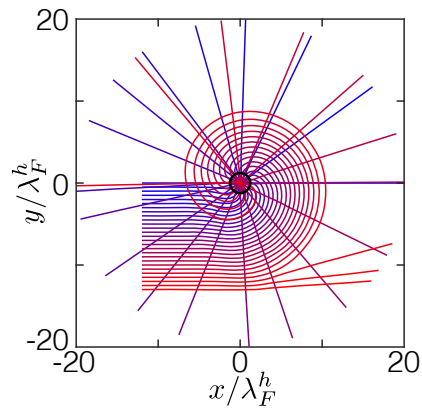


Fig. S1: **Numerical simulation of walker-well interactions.** Simulated trajectories with uniformly-distributed impact parameters y_i for a drop with speed $v_0 = 4.4 \text{ mm s}^{-1}$ at $\gamma/\gamma_F = 0.990$.

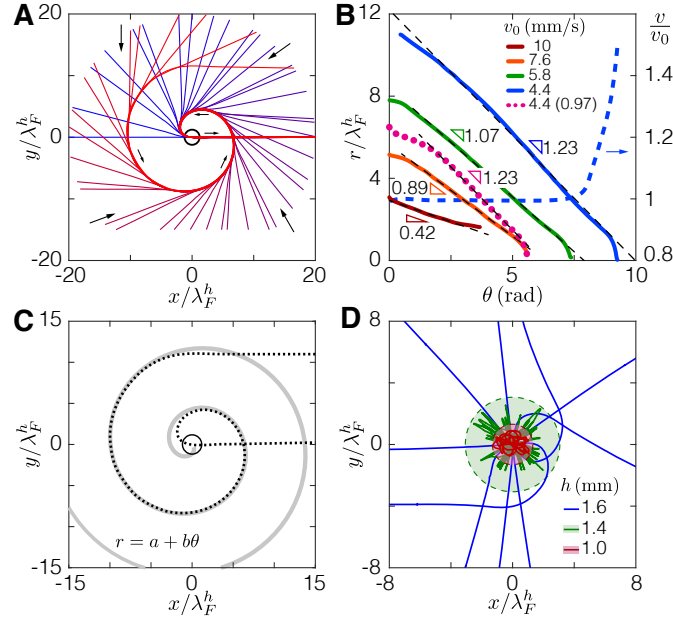


Fig. S2: Spiral trajectory and effective force. **(A)** Unique spiral resulting from suitable rotation of the trajectories shown in Fig. 2D,E and Fig. S1. Only walkers drawn into the well are considered. **(B)** Dependence of the radial coordinate r (solid and dotted lines) on the azimuthal angle θ for the longest spirals achieved with walkers of different size (speed), as previously shown in Fig. 1E. The nearly linear relation between r and θ demonstrates that the incoming drop trajectory is well approximated by an Archimedean spiral. The dashed blue line shows the normalized instantaneous speed v/v_0 corresponding to the drop with speed $v_0 = 4.4 \text{ mm s}^{-1}$ at $\gamma/\gamma_F = 0.990$ (solid blue line). **(C)** Comparison between the drop trajectory (dashed line) and the Archimedean spiral (solid) obtained with the fit shown in **B** for $v_0 = 4.4 \text{ mm s}^{-1}$ at $\gamma/\gamma_F = 0.990$. **(D)** Experimental dependence of walker trajectories at $\gamma/\gamma_F = 0.990$ on depth h illustrates well-induced trapping at small h . The red-shaded area corresponds to the extent of the well. The drop size is the same as in Fig. 1C.

Captions for Supplementary Movies

Movie S1

Oblique view showing a drop walking over the surface of a vibrating fluid bath and interacting with a submerged circular well. Acquisition frame rate: 34 Hz. Video length: 24 seconds.

Movie S2

Experimental drop trajectories in the vicinity of a submerged well, color-coded according to drop speed. Video length: 45 seconds.

Movie S3

Top view illustrating the experimental wave field during the walker-well interaction. The wave field is visualized through a semi-reflective mirror and a diffused-light source. Acquisition frame rate: 17.2 Hz. Video length: 23 seconds.

Movie S4

Top and oblique view illustrating the form of the wave field during the walker-well interaction, as obtained via simulation. Strobings frequency: $f/4$. Video length: 24 seconds.

Movie S5

Top and oblique view illustrating the well-induced wave perturbation during the walker-well interaction, as obtained via simulation. Strobings frequency: $f/4$. Video length: 24 seconds.

The supplementary movies have been recorded in MPEG4 format. Its correct reproduction has been tested with the 'VLC' and 'QuickTime' players on MacOS, and 'VLC' and 'Windows Media' players on PC.

REFERENCES AND NOTES

1. Y. Couder, S. Protière, E. Fort, A. Boudaoud, Dynamical phenomena: Walking and orbiting droplets. *Nature* **437**, 208 (2005).
2. S. Protière, A. Boudaoud, Y. Couder, Particle—wave association on a fluid interface. *J. Fluid Mech.* **554**, 85–108 (2006).
3. J. W. M. Bush, Pilot-wave hydrodynamics. *Annu. Rev. Fluid Mech.* **47**, 269–292 (2015).
4. E. Fort, A. Eddi, A. Boudaoud, J. Moukhtar, Y. Couder, Path-memory induced quantization of classical orbits. *Proc. Natl. Acad. Sci. U.S.A.* **107**, 17515–17520 (2010).
5. A. Eddi, J. Moukhtar, S. Perrard, E. Fort, Y. Couder, Level splitting at macroscopic scale. *Phys. Rev. Lett.* **108**, 264503 (2012).
6. S. Perrard, M. Labousse, M. Miskin, E. Fort, Y. Couder, Self-organization into quantized eigenstates of a classical wave-driven particle. *Nat. Commun.* **5**, 3219 (2014).
7. M. Durey, P. A. Milewski, J. W. M. Bush, Dynamics, emergent statistics, and the mean-pilot-wave potential of walking droplets. *Chaos* **28**, 096108 (2018).
8. D. M. Harris, J. Moukhtar, E. Fort, Y. Couder, J. W. M. Bush, Wavelike statistics from pilot-wave dynamics in a circular corral. *Phys. Rev. E* **88**, 011001 (2013).
9. P. J. Sáenz, T. Cristea-Platon, J. W. M. Bush, Statistical projection effects in a hydrodynamic pilot-wave system. *Nat. Phys.* **14**, 315–319 (2018).
10. T. Cristea-Platon, P. J. Sáenz, J. W. M. Bush, Walking droplets in a circular corral: Quantisation and chaos. *Chaos* **28**, 096116 (2018).
11. M. F. Crommie, C. P. Lutz, D. M. Eigler, Confinement of electrons to quantum corrals on a metal surface. *Science* **262**, 218–220 (1993).

12. H. C. Manoharan, C. P. Lutz, D. M. Eigler, Quantum mirages formed by coherent projection of electronic structure. *Nature* **403**, 512–515 (2000).
13. A. Eddi, E. Sultan, J. Moukhtar, E. Fort, M. Rossi, Y. Couder, Information stored in Faraday waves: The origin of a path memory. *J. Fluid Mech.* **674**, 433–463 (2011).
14. J. W. M. Bush, Y. Couder, T. Gilet, P. A. Milewski, A. Nachbin, Introduction to focus issue on hydrodynamic quantum analogs. *Chaos* **28**, 096001 (2018).
15. G. A. Fiete, E. J. Heller, *Colloquium*: Theory of quantum corrals and quantum mirages. *Rev. Mod. Phys.* **75**, 933–948 (2003).
16. J. Friedel, Electronic structure of primary solid solutions in metals. *Adv. Phys.* **3**, 446–507 (1954).
17. K. Kanisawa, M. J. Butcher, H. Yamaguchi, Y. Hirayama, Imaging of Friedel oscillation patterns of two-dimensionally accumulated electrons at epitaxially grown InAs(111)A surfaces. *Phys. Rev. Lett.* **86**, 3384–3387 (2001).
18. M. Faraday, On a peculiar class of acoustical figures; and on certain forms assumed by groups of particles upon vibrating elastic surfaces. *Philos. Trans. R. Soc. Lond.* **121**, 299–340 (1831).
19. J. Moláček, J. W. M. Bush, Drops walking on a vibrating bath: Towards a hydrodynamic pilot-wave theory. *J. Fluid Mech.* **727**, 612–647 (2013).
20. A. U. Oza, E. Siefert, D. M. Harris, J. Molacek, J. W. M. Bush, Orbiting pairs of walking droplets: Dynamics and stability. *Phys. Rev. Fluids* **2**, 053601 (2017).
21. J. Arbelaiz, A. U. Oza, J. W. M. Bush, Promenading pairs of walking droplets: Dynamics and stability. *Phys. Rev. Fluids* **3**, 013604 (2018).
22. L. Tadrif, J.-B. Shim, T. Gilet, P. Schlagheck, Faraday instability and subthreshold Faraday waves: Surface waves emitted by walkers. *J. Fluid Mech.* **848**, 906–945 (2018).

23. D. M. Harris, P.-T. Brun, A. Damiano, L. M. Faria, J. W. M. Bush, The interaction of a walking droplet and a submerged pillar: From scattering to the logarithmic spiral. *Chaos* **28**, 096105 (2018).
24. L. M. Faria, A model for faraday pilot waves over variable topography. *J. Fluid Mech.* **811**, 51–66 (2017).
25. P. W. Milonni, J. H. Eberly, *Laser Physics* (Wiley, 2010).
26. D. M. Harris, J. W. M. Bush, Droplets walking in a rotating frame: From quantized orbits to multimodal statistics. *J. Fluid Mech.* **739**, 444–464 (2014).
27. Ø. Wind-Willassen, J. Molacek, D. M. Harris, J. W. M. Bush, Exotic states of bouncing and walking droplets. *Phys. Fluids* **25**, 082002 (2013).
28. V. Bacot, S. Perrard, M. Labousse, Y. Couder, E. Fort, Multistable free states of an active particle from a coherent memory dynamics. *Phys. Rev. Lett.* **122**, 104303 (2019).
29. T. Gilet, Dynamics and statistics of wave-particle interactions in a confined geometry. *Phys. Rev. E* **90**, 052917 (2014).
30. T. Gilet, Quantumlike statistics of deterministic wave-particle interactions in a circular cavity. *Phys. Rev. E* **93**, 042202 (2016).
31. M. Durey, P. A. Milewski, Z. Wang, Faraday pilot-wave dynamics in a circular corral. *J. Fluid. Mech.* **891**, A3 (2020).
32. P. W. Anderson, Absence of diffusion in certain random lattices. *Phys. Rev.* **109**, 1492–1505 (1958).
33. M. Imada, A. Fujimori, Y. Tokura, Metal-insulator transitions. *Rev. Mod. Phys.* **70**, 1039–1263 (1998).
34. D. M. Harris, T. Liu, J. W. M. Bush, A low-cost, precise piezoelectric droplet-on-demand generator. *Exp. Fluids* **56**, 83 (2015).

35. D. M. Harris, J. W. M. Bush, Generating uniaxial vibration with an electrodynamic shaker and external air bearing. *J. Sound Vib.* **334**, 255–269 (2015).
36. S. Douady, Experimental study of the Faraday instability. *J. Fluid Mech.* **221**, 383–409 (1990).
37. P. A. Milewski, C. A. Galeano-Rios, A. Nachbin, J. W. M. Bush, Faraday pilot-wave dynamics: Modelling and computation. *J. Fluid Mech.* **778**, 361–388 (2015).
38. N. Sungar, L. D. Tambasco, G. Pucci, P. J. Saenz, J. W. M. Bush, Hydrodynamic analog of particle trapping with the Talbot effect. *Phys. Rev. Fluids* **2**, 103602 (2017).
39. L. D. Tambasco, J. J. Pilgram, J. W. M. Bush, Bouncing droplet dynamics above the Faraday threshold. *Chaos* **28**, 096107 (2018).
40. L. D. Tambasco, J. W. M. Bush, Exploring orbital dynamics and trapping with a generalized pilot-wave framework. *Chaos* **28**, 096115 (2018).